

Resonant exciton second-harmonic generation in self-assembled ZnO microcrystallite thin films

This article has been downloaded from IOPscience. Please scroll down to see the full text article.

2003 J. Phys.: Condens. Matter 15 5191

(<http://iopscience.iop.org/0953-8984/15/30/301>)

View [the table of contents for this issue](#), or go to the [journal homepage](#) for more

Download details:

IP Address: 171.66.16.121

The article was downloaded on 19/05/2010 at 14:21

Please note that [terms and conditions apply](#).

Resonant exciton second-harmonic generation in self-assembled ZnO microcrystallite thin films

X Q Zhang^{1,3}, Z K Tang¹, M Kawasaki², A Ohtomo² and H Koinuma²

¹ Department of Physics, The Hong Kong University of Science and Technology, Clear Water Bay, Kowloon, Hong Kong, People's Republic of China

² Materials and Structures Laboratory, Tokyo Institute of Technology, Nagatsuda, Midori-ku, Yokohama 227, Japan

E-mail: xqzhang@center.njtu.edu.cn

Received 17 February 2003, in final form 3 June 2003

Published 18 July 2003

Online at stacks.iop.org/JPhysCM/15/5191

Abstract

Second-harmonic generation has been studied for fundamental wavelengths from 720 to 1100 nm on high-quality ZnO thin films deposited on sapphire substrates by laser molecular beam epitaxy. The second-order nonlinear susceptibility components increase dramatically as the second-harmonic frequency approaches the ZnO bandgap. The increase is most likely due to a resonance of the second-harmonic frequency with the critical point transition associated with the direct bandgap transition. Large second-order nonlinear susceptibility components were determined to have a nonresonant background value of -83.7 pm V^{-1} for d_{33} , 14.7 pm V^{-1} for d_{31} and 15.2 pm V^{-1} for d_{15} for a fundamental wavelength of 1064 nm. The value of d_{33} for the film was as high as 14 times that of bulk material in the nonresonant region. The difference in values between the second nonlinear coefficients of the bulk and the film may originate from the microcrystallite structure.

For optical storage and information processing, compact short-wavelength coherent light sources are required. Recently, blue–green and blue light-emitting laser diodes based on ZnSe and GaN were demonstrated [1–4]. However, these lasers are still at the experimental stage, so it is advisable to also think about other techniques for attaining this target. Nonlinear optics offers the possibility of doubling the light frequency of already well-developed near-infrared laser diodes. Wide-bandgap II–VI semiconductors are promising materials for efficient second-harmonic generation (SHG), since they possess strong second-order nonlinear susceptibilities $\chi^{(2)}$. Their large bandgaps allow frequency doubling into the blue spectral region without absorption. Furthermore, high-quality single-crystalline II–VI compound

³ Permanent address: Institute of Optoelectronic Technology, Northern Jiaotong University, Beijing 100044, People's Republic of China.

semiconductor films can be grown using modern growth techniques such as metal organic vapor phase epitaxy [5] and molecular beam epitaxy [6–8].

For frequencies near the exciton resonance, the large and interesting effects of spatial dispersion on the linear optical properties are well known and have been studied extensively. In contrast, significant effects of the exciton spatial dispersion on the nonlinear optical properties have not been demonstrated clearly. Additionally, ZnO has a large bandgap energy and is therefore suited to short-wavelength applications. Despite this potential, little is known about its nonlinear optical properties. For this reason, in this paper we report the frequency-dependent measurement of the second-order optical nonlinearities of ZnO thin films deposited on sapphire substrates by laser molecular beam epitaxy (L-MBE) for fundamental wavelengths in the range 720–1100 nm using an optical parametric amplifier (OPA) system, which increase dramatically as the second-harmonic wavelengths approach the edge of the ZnO bandgap. The magnitude of the second-order nonlinear susceptibility component d_{33} is determined to have a uniform value of -83.7 pm V^{-1} for the fundamental wavelength 1064 nm in a ZnO thin film with a thickness of 44.4 nm. This is about 14 times the value for bulk ZnO [9]. The difference between the values of the second-order nonlinear coefficients for bulk and film may originate from the microcrystallite structure.

Second-order nonlinear susceptibilities for bulk ZnO have been reported by some research groups [8–10]. In this work, self-assembled high-quality ZnO microcrystallites were grown on sapphire substrates using the L-MBE technique [11] at a deposition temperature of 500 °C and an oxygen pressure of 1×10^{-6} Torr. A pure ceramic ZnO target (99.999%) was ablated in an ultra-high-vacuum chamber using a KrF excimer laser. A reflection high-energy electron diffraction pattern showed well-defined streaks at the initial growth stage. An x-ray diffraction measurement revealed that the ZnO microcrystallites have high crystallinity with *c*-axis orientation. The atomic force microscope topography show that the thin films consist of close-packed hexagons. The hexagonal column structure is also confirmed by transmission electron microscope observations [6]. The facets of the hexagons correspond to the {1100} plane and they are strictly parallel to the {1120} plane of the sapphire substrate.

SHG properties were studied for fundamental wavelengths in the range of 720–1100 nm from an OPA [12, 13], which was pumped by the frequency-tripled output of a Q-switched, mode-locked Nd:YAG laser with a pulse duration of 35 ps and a repetition rate of 10 Hz at a wavelength of 355 nm. The OPA output was continuously tunable between 400 and 2000 nm. The second harmonic was measured in transmission. The laser beam is split so that the second-harmonic intensities from the sample (I_s) and from a Y-cut quartz wedge (I_0), as in [14, 15], can be measured simultaneously. To eliminate the influence of the frequency dependence of the OPA output as well as laser power fluctuations, the sample-to-reference intensity ratio (I_s/I_0) was taken to be the measured result. The polarization of the fundamental beam could be changed by rotating a half-wave plate placed in front of the sample. Glass filters were used to remove either the idler or the signal component of the OPA output. Wide-band filters were placed after the sample to ensure that only the second-harmonic intensities were measured. The polarization of the second-harmonic signal was checked using a linear polarizer placed behind the filter. The thin film normal is tilted 45° to the incident laser beam. Finally, the intensities of SHG from the ZnO film and that from the quartz wedge are detected by two identical monochrometers and photomultiplier tubes, averaged by a box-car integrator, and then recorded by a computer. Ensuring uniform spectral response in the two detection arms, the spectral responses of the reference and sample arms include the effects of the spectral response of the identical glass filters, monochrometers, and photomultiplier tubes in each arm.

To determine the absolute value of the $\chi^{(2)}$ of a sample, the relative SHG signal is calibrated against that generated in a Y-cut quartz plate placed at the same location as the sample and

oriented at a peak in the Marker fringe pattern. Since the dispersion of $\chi^{(2)}$ in quartz is negligible in the wavelength range involved, it is sufficient to make the calibration at one wavelength.

To deduce the second-order nonlinear coefficients of ZnO thin films, the SHG data were analysed with the assumption that absorption was negligible at the fundamental but not at the second-harmonic wavelengths. The linear absorption in these films is only significant near the bandgap. For a ZnO film with a thickness much less than the coherence length, the intensity of SHG was measured and compared to SHG from a quartz wedge. The ratio of the intensities of the SHG from the ZnO film and the Y-cut quartz wedge is given by

$$\frac{I_s(2\omega)}{I_q(2\omega)} = \left[\frac{l^2 \pi^2}{2l_c^2} \right] \left[\frac{n_q^2(\omega)n_q(2\omega)}{n_s^2(\omega)n_s(2\omega)\cos^2(\theta)} \right] \left[\frac{4e^{-\beta l}(1 - e^{\beta l/2})^2}{(\beta l)^2} \right] \left[\frac{\chi_{\text{eff}}^{(2)}(\theta)}{\chi_q^{(2)}} \right]^2 \quad (1)$$

where β is the linear absorption coefficient at the second-harmonic wavelength, l_c is the quartz coherence length, $\chi_{\text{eff}}^{(2)}$ is the measured effective second-order nonlinear optical susceptibility, $n(\omega)$ and $n(2\omega)$ are the index of refraction at frequencies ω and 2ω , respectively, $l_c = 20 \mu\text{m}$ is the coherent length of the quartz, and l is the film thickness.

For hexagonal materials with 6 mm symmetry, the effective second-order nonlinear susceptibility of p-polarized SHG versus the fundamental wave polarization angle α at an incidence angle of $\sim 45^\circ$ is given by [16–18]

$$\chi_{\text{eff p}}^{(2)}(\alpha) = 2[d_{31} \sin^2 \alpha + (2d_{15} \sin \theta \cos \theta + d_{31} \cos^2 \theta + d_{33} \sin^2 \theta) \cos^2 \alpha]^2. \quad (2)$$

The effective second-order nonlinear susceptibility of s-polarized SHG versus the fundamental wave polarization angle α at an incidence angle of $\sim 45^\circ$ is given by

$$\chi_{\text{eff s}}^{(2)}(\alpha) = 4d_{15}^2 \sin^2 2\alpha \sin^2 \theta \quad (3)$$

where d_{33} , d_{31} and d_{15} are the second-order nonlinear susceptibilities, respectively.

The polarization dependence of the second harmonic of $1.064 \mu\text{m}$ incident light in ZnO films was measured at room temperature for an incidence angle of $\sim 45^\circ$. Figure 1 shows a plot of the p-polarized transmitted SH intensity in a ZnO thin film with a thickness of 44.4 nm versus the input polarization angle of the incident fundamental light, where the solid squares represent the experimental data and the solid curve is a fit to equation (2). As shown in figure 1, the fit was quite good. As shown in figure 2, the polarization dependence of the s-polarized transmitted SH intensity of $1.064 \mu\text{m}$ incident light could also be fitted well using equation (3).

Equation (1) can therefore be applied to determine d_{33} , d_{31} and d_{15} as a function of dq_{11} , the second-order nonlinear coefficient for quartz ($dq_{11} = 0.3 \text{ pm V}^{-1}$). For the ZnO thin film, the second-order nonlinear coefficients are found to be $d_{33} = -83.7 \text{ pm V}^{-1}$, $d_{31} = 14.7 \text{ pm V}^{-1}$ and $d_{15} = 15.2 \text{ pm V}^{-1}$. The nonzero second-order optical nonlinear coefficients of bulk ZnO are reported to be $d_{33} = -5.86 \text{ pm V}^{-1}$, $d_{31} = 1.76 \text{ pm V}^{-1}$ and $d_{15} = 1.93 \text{ pm V}^{-1}$ [9, 19]. Compared with bulk crystal ZnO, we find that the d_{33} in film increases by about 14 times. This tremendous difference may originate from the difference in the microcrystallite structure. The second-order nonlinear coefficients were enhanced significantly by the effect of grain and grain boundaries. In the thin films, the grain crystallites have close-packed hexagonal column structure. There are no domain walls in the z direction. This will increase the macroscopic effect of the second-order process [8, 20, 21].

The second-order nonlinear coefficients are different in ZnO thin films of different qualities. For ZnO thin film with a thickness of 45 nm deposited on sapphire substrates by pulsed laser ablation, Cao *et al* [8] reported second-order nonlinear coefficients of 6.7 pm V^{-1} for d_{33} and 1.8 pm V^{-1} for d_{31} , which are close to the values in the bulk. In our sample, x-ray diffraction measurement revealed that the ZnO microcrystallites have high crystallinity with a c -axis orientation. The atomic force microscope topography showed that the thin films

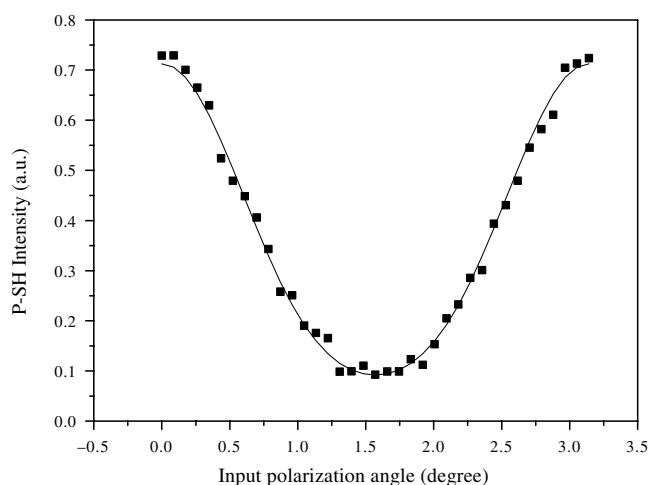


Figure 1. Experimental and theoretical plots of the p-polarized second-harmonic signal intensity versus the polarization of the incident light. The solid squares are the experimental points. The solid curve corresponds to a theoretical fit.

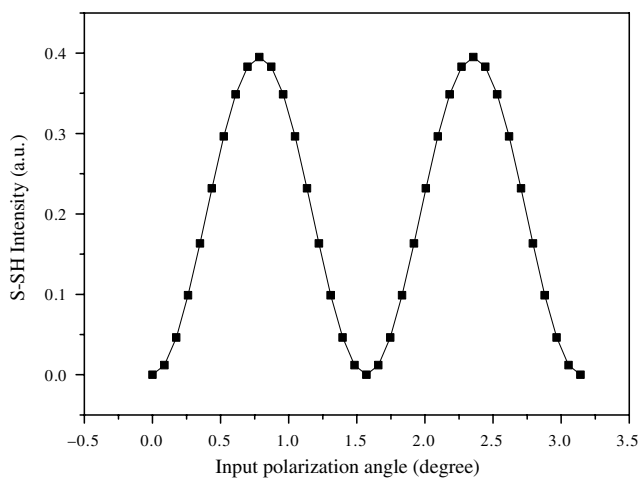


Figure 2. The s-polarized second-harmonic signal intensity versus the polarization of the incident light. The solid squares are the experimental points. The solid curve corresponds to a theoretical fit.

consisted of close-packed hexagons. The hexagonal column structure is also confirmed by transmission electron microscope observation [6]. The facets of the hexagons correspond to the $\{1100\}$ plane, and they are strictly parallel to the $\{1120\}$ plane of the sapphire substrate. The crystallinity of the ZnO microcrystallite thin films is improved, thus the magnitude of the second-order nonlinear coefficients may be further increased.

Figure 3(a) shows the absorption spectra in the ZnO thin film at room temperature. The microcrystallite ZnO thin film shows a clear exciton absorption peak at 3.34 eV even at room temperature, indicating the excellent quality of the sample. Compared with the band-edge absorption near 3.4 eV, this exciton absorption shows that the exciton binding energy is in the 60 meV range for this microcrystallite ZnO thin film. The energy dependence of the refractive

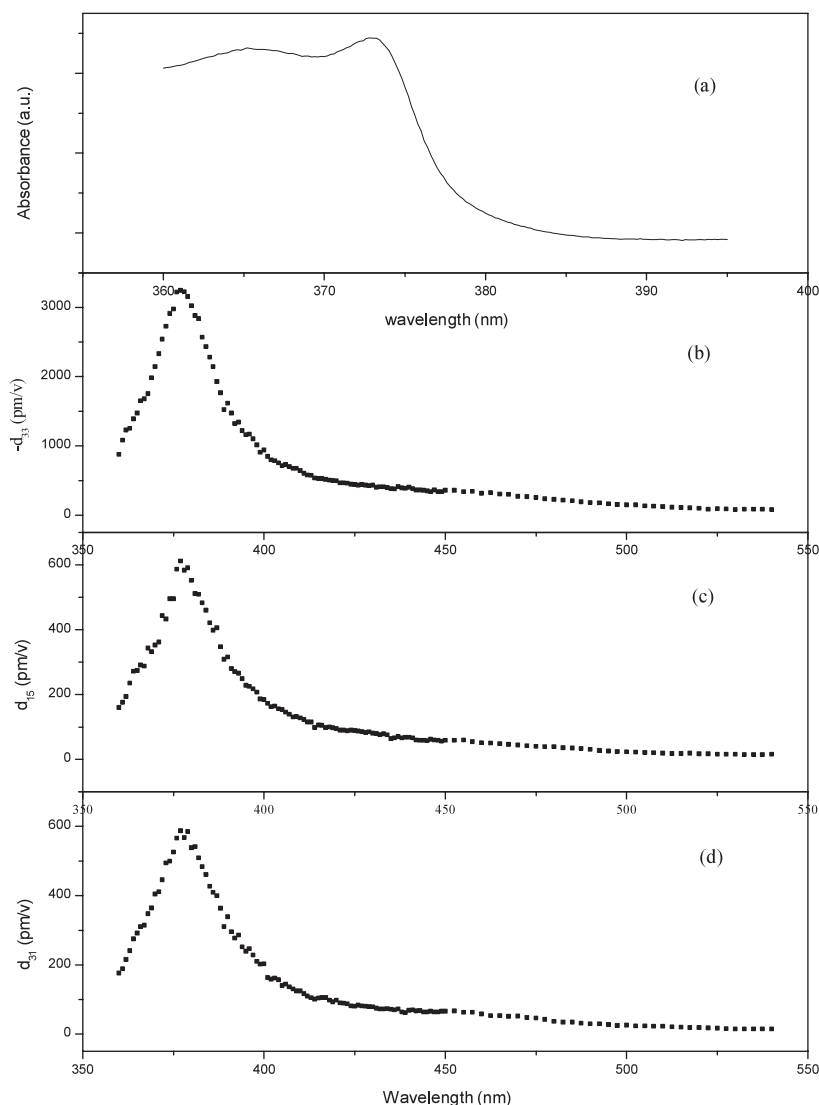


Figure 3. (a) Absorption spectra in ZnO thin film at room temperature. (b), (c) and (d) Second-order nonlinear susceptibility components as a function of the second-harmonic wavelength for ZnO thin film at room temperature.

index for ZnO is taken from [22]. From the SHG data in the excitonic region, its resonance behaviour can be obtained. The deduced d_{33} , d_{31} and d_{15} values are plotted as a function of SHG wavelength in figures 3(b)–(d), respectively. An almost uniform background value characterizes the second-order response from the SHG wavelength at 400 nm and longer. Below this wavelength the response appears to be resonant in nature, increasing rapidly as the bandgap is approached. This increase is most probably due to a resonance of the second-harmonic frequency with the critical point transition associated with the direct bandgap transition.

In conclusion, we have measured the wavelength dependence of the SHG from ZnO thin films deposited on sapphire substrates by L-MBE at fundamental wavelengths from 720 to 1100 nm. Second-order nonlinear susceptibility components are substantial over this

wavelength range and increase dramatically as the second-harmonic frequency approaches the edge of the bandgap. This is most probably due to resonance of the second-harmonic frequency with the critical point transition associated with the direct bandgap of the ZnO thin film. The magnitude of the second-order nonlinear susceptibility components d_{33} is determined to have a uniform value of -83.7 pm V^{-1} for fundamental wavelengths in the infrared region. This is 14 times the value of bulk ZnO. The different values of the second-order nonlinear coefficients for bulk and film may result from the microcrystallite structure. The second-order nonlinear coefficients were enhanced significantly by the effect of grain and grain boundaries. These results demonstrate that the ZnO thin films prepared by L-MBE are very promising candidates for short-wavelength nonlinear optical device applications.

Acknowledgments

This work was supported by CERG grants from the Research Grants Committee of Hong Kong, the Lightwave Technology Research Programmer of the Hong Kong Techcom of Information Technology, the National Natural Science Foundation of China, and the Foundation of Northern Jiaotong University (PD 213). The authors would like to thank Professor G K L Wong for helpful discussions.

References

- [1] Haase M A, Qui J, Depuydt J M and Cheng H 1991 *Appl. Phys. Lett.* **59** 1272
- [2] Nakamura S, Senoh M, Nakahana S, Iwasa N, Yama T, Matsushita T, Sugimoto Y and Kiyoku H 1996 *Appl. Phys. Lett.* **69** 1477
- [3] Wiesmann D, Brener I, Pfeiffer L, Khan M A and Sun C J 1996 *Appl. Phys. Lett.* **69** 3384
- [4] Nakamura S, Senoh M, Nakahana S, Iwasa N, Yama T, Matsushita T, Sugimoto Y and Kiyoku H 1997 *Appl. Phys. Lett.* **70** 2753
- [5] Kuhn W, Naumov A, Stanzl H, Bauer S, Wolf K, Wanger H P, Gebhardt W, Pohl U W, Krost A, Richter W, Dumichen U and Thiele K H 1995 *J. Cryst. Growth* **123** 605
- [6] Tang Z K, Yu P, Wong G K L, Kawasaki M, Chitomo A, Koinuma H and Segawa Y 1998 *Appl. Phys. Lett.* **72** 3270
- [7] Bagnall D M, Chen Y F, Zhu Z, Yao T, Koyama S, Shen M Y and Goto T 1997 *Appl. Phys. Lett.* **70** 2230
- [8] Cao H, Wu J Y, Ong H C, Dai J Y and Chang R P H 1998 *Appl. Phys. Lett.* **76** 572
- [9] Miller R C and Nordland W A 1970 *Opt. Commun.* **1** 400
- [10] Haueisen D C and Mahr H 1973 *Phys. Rev.* **B 8** 734
- [11] Koinuma H and Yoshimoto M 1994 *Appl. Surf. Sci.* **75** 308
- [12] Lundquist P M, Yitzchaik S, Zhang T G, Kanis D, Ratner M A, Tobin J M and Wong G K 1994 *Appl. Phys. Lett.* **64** 2194
- [13] Huang J Y, Zhang J Y, Shen Y R, Chen C and Wu B 1990 *Appl. Phys. Lett.* **57** 1961
- [14] Lotem H, Koren G and Yacoby Y 1974 *Phys. Rev.* **B 9** 3532
- [15] Wynne J J and Bloembergen N 1969 *Phys. Rev.* **188** 1211
- [16] Blanc D, Cachard A and Pommier J 1997 *Opt. Eng.* **36** 1191
- [17] Lin W P, Lundquist P M, Wong G K, Rippert E D and Ketterson J B 1993 *Appl. Phys. Lett.* **63** 2875
- [18] Blanc D, Cachard A, Pommier J C, Roux J F and Coutaz J L 1994 *Opt. Mater.* **3** 41
- [19] Singh S 1986 *Handbook Laser Science and Technology: Part 1 Optical Materials* vol 3 (Boca Raton, FL: Chemical Rubber Company Press)
- [20] Guerrero A and Mendoza Bernardo S 1995 *J. Opt. Soc. Am.* **B 12** 559
- [21] Chang C S and Lue J T 1997 *Surf. Sci.* **393** 231
- [22] Dumont E, Dugnoille B and Bienfait S 1999 *Thin Solid Films* **355** 93